Investigating Fully-Strange Tetraquark System with Positive Parity in a Chiral Quark Model

Yue Tan , Yuheng Wu , Hongxia Huang * , Jialun Ping

Posted Date: 19 October 2023

doi: 10.20944/preprints202310.1221.v1

Keywords: quark model; real scaling method; resonance; Gaussian expansion

Article

Investigating Fully-Strange Tetraquark System with Positive Parity in a Chiral Quark Model

Yue Tan [1], Yuheng Wu [2], Hongxia Huang [2,*] and Jialun Ping [2]

[1] Department of Physics, Yancheng Institute of Technology, Yancheng 224000, P. R. China; tanyue@ycit.edu.cn
[2] Department of Physics, Nanjing Normal University, Nanjing 210023, P.R. China; 191002007@njnu.edu.cn (Y.W.); jlping@njnu.edu.cn (J.P.)
* Correspondence: Hongxia Huang@njnu.edu.cn

Abstract: Motivated by the intriguing discovery of $X(6900)$ by LHCb Collaboration, we undertake a comprehensive study of the $s\bar{s}s\bar{s}$ tetraquark system in positive parity, employing the Gaussian expansion within the chiral quark model method. We consider two structures, diquark-antidiquark (ss-$\bar{s}\bar{s}$) structure and meson-meson ($s\bar{s}$-$s\bar{s}$)strcuture, encompassing all conceivable color and spin configurations. Despite the absence of bound states in our calculations, we have identified potential resonant states with $J^P = 0^+$, namely $R(0, 2150)$ and $R(0, 2915)$, as well as a resonant state with $J^P = 1^+$ denoted as $R(1, 2950)$, and a resonant state with $J^P = 2^+$ denoted as $R(2, 2850)$, utilizing the real-scaling method. Through a comparison of their energies and widths, we propose that $R(0, 2915)$ and $R(1, 2950)$ may share characteristics with $X(6900)$, while $R(0, 2150)$ could be a promising experimental candidate for $f_0(2100)$. We strongly advocate for experimental investigations to shed light on the existence and properties of these resonant states.

Keywords: quark model; real scaling method; resonance; Gaussian expansion

1. Introduction

Since its initial discovery by the Belle Collaboration in 2003 [1], the $X(3872)$ state has garnered significant attention on $c\bar{q}q\bar{c}$ structure. There's a lot of work on $c\bar{q}q\bar{c}$ structure, such as $Y(4260)$ [2], $Z_c(3900)$ [3], $Y(4660)$ [4], and so on. Now, researchers have extensively investigated various structures involving heavy quarks and antiquarks, denoted by $Q\bar{q}q\bar{Q}$, within exotic tetraquark states. Examples include the possibility of $Y(4274)$ as a $c\bar{s}s\bar{c}$ structure, $D^*_{s0}(2317)$ as a $c\bar{q}q\bar{s}$ configuration, and $\Upsilon(10753)$ as a $b\bar{q}q\bar{b}$ state, which can be found in Refs.[5–7]. These studies have significantly contributed to a deeper understanding of QCD. Recent observations by the LHCb Collaboration have added to the rich landscape of exotic states with the discovery of the $X(6900)$ resonance in the di-J/ψ invariant mass spectrum [8]. Subsequent reports from CMS and ATLAS Collaborations have highlighted additional resonances, such as $X(6200)$, $X(6600)$, and $X(7200)$, sparking renewed theoretical interest in exotic states with the $Q\bar{Q}Q\bar{Q}$ configuration [9,10]. However, investigations into resonance states within the $s\bar{s}s\bar{s}$ configuration, particularly focusing on the tetraquark state with positive parity, are currently limited in the literature.

Studies of the $s\bar{s}s\bar{s}$ configuration may be traced back to discovery of $Y(2175)$ in 2006 [11], which is now known as $\phi(2170)$, in the initial state-radiation (ISR) process of $e^+e^- \to \gamma_{ISR}\phi\pi^+\pi^-$. The mass of this state is measured to be 2163 ± 7 MeV with a width of 103^{+28}_{-21} MeV. More recently, the BESIII Collaboration reported the observation of a new structure, $X(2100)$, in the $\phi\eta^{'}$ mass spectrum [12]. The quantum numbers of $X(2063)$ are still under investigation. If $J^P = 1^+$, the mass is determined to be $2062.8 \pm 13.1 \pm 4.2$ MeV with a width of $177 \pm 36 \pm 20$ MeV. Alternatively, if $J^P = 1^-$, the mass is estimated to be $2002.1 \pm 27.5 \pm 15.0$ MeV with a width of 103^{+28}_{-21} MeV. Furthermore, recent reports from the BESIII Collaboration have shed light on two distinct resonances: $X(2500)$ observed in the context of $J/\psi \to \gamma\phi\phi$ [13], and the recently discovered $X(2239)$ resonance within the $e^+e^- \to K^+K^-$ process [14]. These discoveries have significantly expanded the $s\bar{s}s\bar{s}$ family. However, as of yet, the existence of clear positive parity $s\bar{s}s\bar{s}$ states remains elusive.

Preprints (www.preprints.org) | NOT PEER-REVIEWED | Posted: 19 October 2023 doi:10.20944/preprints202310.1221.v1

Current theoretical research is prominently focused on the $s\bar{s}s\bar{s}$ tetraquark state, particularly exploring its negative parity aspects. In Ref.[15], the author presented standard criteria within the QCD sum rules approach and conducted a comprehensive phenomenological analysis. The author suggests that $Y(2175)$ potentially may consist of color octet constituents rather than diquark pairs. Similarly, in Ref.[16], Chen et al. employed the QCD sum rule framework, constructing both diquark-antidiquark currents $(ss)(\bar{s}\bar{s})$ and meson-meson currents $(s\bar{s})(s\bar{s})$. They extensively studied the decay properties of $Y(2175)$. Based on this work, Chen et al. recently utilized two independent $ss\bar{s}\bar{s}$ interpolating currents with $J^{PC} = 1^{--}$, calculating both their diagonal and off-diagonal correlation functions. This calculation yielded two distinct physical states, one being $Y(2175)$ and the other at an energy level near 2.41 GeV, consistent with recent experimental observations [17]. Additionally, researchers investigated the mass spectrum of the $ss\bar{s}\bar{s}$ tetraquark states within the relativized quark model, incorporating screening effects. Notably, the observed resonance at 2239 MeV could potentially correspond to a wave 1^{--} $ss\bar{s}\bar{s}$ tetraquark state [18]. On the other hand, studies pertaining to the $ss\bar{s}\bar{s}$ tetraquark state with positive parity have also made significant progress. Deng et al. utilized a chiral quark model to calculate the properties of the efficient $ss\bar{s}\bar{s}$ tetraquark state. Their results indicated that the 0^+ state had an energy of approximately 1925 MeV, suggesting a candidate for $f_0(2020)$ [19]. In the QCD sum rule framework (Chen et al., Refs.[20,21]), calculations for quantum numbers 0^{++}, 1^{+-}, 2^{++} of the $ss\bar{s}\bar{s}$ four-quark state were conducted, yielding energies around 2.0 GeV. Additionally, quantum numbers 0^{-+} and 2^{-+} were associated with energies approximately $2.45^{+0.20}_{-0.24}$ GeV and $3.07^{+0.25}_{-0.33}$ GeV, respectively. The energy of the 1^{+-} tetraquark state aligned with results available in the literature [22,23].

In this study, we employ the Gaussian Expansion Method (GEM) to investigate the tetraquark system of $s\bar{s}s\bar{s}$ with quantum numbers of $0^+, 1^+, 2^+$ within the framework of a chiral quark model. Two distinct structures are considered in our calculations: the $s\bar{s}$-$s\bar{s}$ molecular structure and the ss-$\bar{s}\bar{s}$ diquark structure. In theory, all energy levels within the diquark structure and color-octet structure are expected to be bound states. However, in practice, only a limited number of structures are observed experimentally. Hence, it is imperative to couple the diquark structure with the molecular structure to investigate whether the structures produced by these diquarks decay into the molecular structures. Additionally, our calculations are conducted within a finite space, potentially resulting in energy levels that may not accurately represent the true resonance states. To address this concern, we introduce the real-scaling method in this paper. This work applies the real-scaling method to test and find resonant states below 3 GeV based on the experimental and theoretical evidence that the energies of the discovered resonant states with $s\bar{s}s\bar{s}$ configuration are all lower than 3 GeV.

The structure of this paper is organized as follows: In Section I, we provide an introduction to the study. In Section II, we elaborate on the details of the Chiral Quark Model (ChQM) and Gaussian Expansion Method (GEM) employed in our investigation. Subsequently, in Section III, we describe a method for identifying and calculating the decay width of the genuine resonance state. In Section IV, we present the numerical results. Finally, in Section IV, we summarize our findings and conclude this work.

2. Chiral quark model, wave function of $s\bar{s}s\bar{s}$ system

2.1. Chiral quark model

The chiral quark model, a well-established theoretical framework renowned for its success in describing hadron spectra and hadron-hadron interactions, has been instrumental in shaping our approach in this study. Interested readers are encouraged to refer to the comprehensive details of the

Preprints (www.preprints.org) | NOT PEER-REVIEWED | Posted: 19 October 2023 doi:10.20944/preprints202310.1221.v1

model available in Refs. [24–26]. Here only the Hamiltonian of the chiral quark model for four-quark system is shown,

$$\begin{aligned} H &= \sum_{i=1}^{n}(m_i + \frac{p_i^2}{2m_i} - T_{CM}) + \sum_{i<j=1}^{n}[V_{con}(r_{ij}) \\ &+ V_{oge}(r_{ij}) + \sum_{\chi=\pi,\eta,K} V_\chi(r_{ij})], \end{aligned} \tag{1}$$

where m_i is the constituent masse of i-th quark (antiquark), and μ is the reduced masse of two interacting quarks or quark-clusters.

$$\begin{aligned} \mu_{ij} &= \frac{m_i m_j}{m_i + m_j}, \ ij = 12, 34 \\ \mu_{1234} &= \frac{(m_1 + m_2)(m_3 + m_4)}{m_1 + m_2 + m_3 + m_4}, \\ p_{ij} &= \frac{m_j p_i - m_i p_j}{m_i + m_j}, \\ p_{1234} &= \frac{(m_3 + m_4)p_{12} - (m_1 + m_2)p_{34}}{m_1 + m_2 + m_3 + m_4}. \end{aligned} \tag{2}$$

$V_{con}(r_{ij})$ is the confining potential, mimics the “confinement" property of QCD,

$$V_{con}(r_{ij}) = (-a_c r_{ij}^2 - \Delta)\boldsymbol{\lambda}_i^c \cdot \boldsymbol{\lambda}_j^c \tag{3}$$

The second potential $V_{oge}(r_{ij})$ is one-gluon exchange interaction reflecting the “asymptotic freedom" property of QCD.

$$\begin{aligned} V_{oge}(r_{ij}) &= \frac{\alpha_s}{4}\boldsymbol{\lambda}_i^c \cdot \boldsymbol{\lambda}_j^c \left[\frac{1}{r_{ij}} - \frac{2\pi}{3m_i m_j}\boldsymbol{\sigma}_i \cdot \boldsymbol{\sigma}_j \delta(\boldsymbol{r}_{ij})\right] \\ \delta(\boldsymbol{r}_{ij}) &= \frac{e^{-r_{ij}/r_0(\mu_{ij})}}{4\pi r_{ij} r_0^2(\mu_{ij})}, \end{aligned} \tag{4}$$

$\boldsymbol{\sigma}$ are the $SU(2)$ Pauli matrices; $\boldsymbol{\lambda}_c$ are $SU(3)$ color Gell-Mann matrices, $r_0(\mu_{ij}) = \frac{r_0}{\mu_{ij}}$ and α_s is an effective scale-dependent running coupling,

$$\alpha_s(\mu_{ij}) = \frac{\alpha_0}{\ln\left[(\mu_{ij}^2 + \mu_0^2)/\Lambda_0^2\right]}. \tag{5}$$

Preprints (www.preprints.org) | NOT PEER-REVIEWED | Posted: 19 October 2023 doi:10.20944/preprints202310.1221.v1

The third potential $V_\chi(r_{ij})$ is Goldstone boson exchange, coming from "chiral symmetry spontaneous breaking" of QCD in the low-energy region,

$$\begin{aligned}
V_\pi(r_{ij}) &= \frac{g_{ch}^2}{4\pi}\frac{m_\pi^2}{12m_im_j}\frac{\Lambda_\pi^2}{\Lambda_\pi^2-m_\pi^2}m_\pi v_{ij}^\pi\sum_{a=1}^{3}\lambda_i^a\lambda_j^a,\\
V_K(r_{ij}) &= \frac{g_{ch}^2}{4\pi}\frac{m_K^2}{12m_im_j}\frac{\Lambda_K^2}{\Lambda_K^2-m_K^2}m_K v_{ij}^K\sum_{a=4}^{7}\lambda_i^a\lambda_j^a,\\
V_\eta(r_{ij}) &= \frac{g_{ch}^2}{4\pi}\frac{m_\eta^2}{12m_im_j}\frac{\Lambda_\eta^2}{\Lambda_\eta^2-m_\eta^2}m_\eta v_\eta \\
&\quad \left[\lambda_i^8\lambda_j^8\cos\theta_P-\lambda_i^0\lambda_j^0\sin\theta_P\right],\\
V_\sigma(r_{ij}) &= -\frac{g_{ch}^2}{4\pi}\frac{\Lambda_\sigma^2}{\Lambda_\sigma^2-m_\sigma^2}m_\sigma\left[Y(m_\sigma r_{ij})-\frac{\Lambda_\sigma}{m_\sigma}Y(\Lambda_\sigma r_{ij})\right],\\
v_{ij}^\chi &= \left[Y(m_\chi r_{ij})-\frac{\Lambda_\chi^3}{m_\chi^3}Y(\Lambda_\chi r_{ij})\right]\boldsymbol{\sigma}_i\cdot\boldsymbol{\sigma}_j,\ \ \chi=\pi,K,\eta,\\
&\quad Y(x)=e^{-x}/x.
\end{aligned}\tag{6}$$

$\boldsymbol{\lambda}$ are $SU(3)$ flavor Gell-Mann matrices, m_χ are the masses of Goldstone bosons, Λ_χ are the cut-offs, $g_{ch}^2/4\pi$ is the Goldstone-quark coupling constant.

All the parameters are determined by fitting the meson spectrum, from light to heavy, taking into account only a quark-antiquark component. They are shown in Table 1.

Table 1. Quark model parameters ($m_\pi=0.7$ fm, $m_\sigma=3.42$ fm, $m_\eta=2.77$ fm, $m_K=2.51$ fm).

Quark masses	$m_u=m_d$(MeV)	313
	m_s(MeV)	536
	m_c(MeV)	1728
	m_b(MeV)	5112
Goldstone bosons	$\Lambda_\pi=\Lambda_\sigma(fm^{-1})$	4.2
	$\Lambda_\eta=\Lambda_K(fm^{-1})$	5.2
	$g_{ch}^2/(4\pi)$	0.54
	$\theta_p(^\circ)$	-15
Confinement	a_c(MeV)	101
	Δ(MeV)	-78.3
	μ_c(MeV)	0.7
OGE	α_0	3.67
	$\Lambda_0(fm^{-1})$	0.033
	μ_0(MeV)	36.976
	$\hat{r}_0$(MeV)	28.17

2.2. The wave function of $s\bar{s}s\bar{s}$ system

There are two physically important structures, meson-meson and diquark-antidiquark, are considered in the present calculation. The wave functions of every structure all consists of four parts: orbital, spin, flavor and color. The wave function of each part is constructed in two steps, first write down the two-body wave functions, then coupling two sub-clusters wave functions to form the

Preprints (www.preprints.org) | NOT PEER-REVIEWED | Posted: 19 October 2023 doi:10.20944/preprints202310.1221.v1

four-body one. Because there are two identical quark pairs in the system, the total wave function for the $s\bar{s}s\bar{s}$ system will be the tensor product of orbital ($|R_i\rangle$), spin ($|S_j\rangle$), color ($|C_k\rangle$) and flavor ($|F_n\rangle$) components with necessary coupling,

$$|ijkn\rangle = \mathcal{A}[|R_i\rangle \otimes |S_j\rangle] \otimes |C_k\rangle \otimes |F_n\rangle. \tag{7}$$

Where $\mathcal{A}$ is the antisymmetrization operator. For the $s\bar{s}s\bar{s}$ system, $\mathcal{A} = 1 - P_{13} - P_{24} + P_{13}P_{24}$.

2.2.1. orbital wave function

The orbital wave function of the four-quark system consists of two sub-cluster orbital wave function and the relative motion wave function between two subclusters (1,3 denote quarks and 2,4 denote antiquarks),

$$\begin{aligned} |R_1\rangle &= \left[[\Psi_{l_1=0}(\mathbf{r}_{12})\Psi_{l_2=0}(\mathbf{r}_{34})]_{l_{12}}\Psi_{L_r}(\mathbf{r}_{1234})\right]_L, \\ |R_2\rangle &= \left[[\Psi_{l_1=0}(\mathbf{r}_{13})\Psi_{l_2=0}(\mathbf{r}_{24})]_{l_{12}}\Psi_{L_r}(\mathbf{r}_{1324})\right]_L, \end{aligned} \tag{8}$$

where the bracket "[ ]" indicates orbital angular momentum coupling, and L is the total orbital angular momentum which comes from the coupling of L_r, orbital angular momentum of relative motion, and l_{12}, which coupled by l_1 and l_2, sub-cluster orbital angular momenta. Given our focus on investigating the tetraquark state of $s\bar{s}s\bar{s}$ with positive parity, we set both l_{12} and L_r to zero. $|R_1\rangle$ donate the orbital wave functions of meson-meson structure, and $|R_2\rangle$ donate the wave functions of diquark-antidiquark structure. In GEM, the radial part of the orbital wave function is expanded by a set of Gaussians:

$$\Psi(\mathbf{r}) = \sum_{n=1}^{n_{\max}} c_n \psi^G_{nlm}(\mathbf{r}), \tag{9a}$$

$$\psi^G_{nlm}(\mathbf{r}) = N_{nl} r^l e^{-\nu_n r^2} Y_{lm}(\hat{\mathbf{r}}), \tag{9b}$$

where N_{nl} are normalization constants,

$$N_{nl} = \left[\frac{2^{l+2}(2\nu_n)^{l+\frac{3}{2}}}{\sqrt{\pi}(2l+1)}\right]^{\frac{1}{2}}. \tag{10}$$

c_n are the variational parameters, which are determined dynamically. The Gaussian size parameters are chosen according to the following geometric progression

$$\nu_n = \frac{1}{r_n^2}, \quad r_n = r_1 a^{n-1}, \quad a = \left(\frac{r_{n_{\max}}}{r_1}\right)^{\frac{1}{n_{\max}-1}}. \tag{11}$$

This procedure enables optimization of the using of Gaussians, as small as possible Gaussians are used.

2.2.2. spin wave function

Because of no difference between spin of quark and antiquark, the meson-meson structure has the same spin wave function as the diquark-antidiquark structure. The spin wave functions of the sub-cluster are shown below.

$$\chi^\sigma_{11} = \alpha\alpha, \ \chi^\sigma_{10} = \frac{1}{\sqrt{2}}(\alpha\beta + \beta\alpha), \ \chi^\sigma_{1-1} = \beta\beta,$$
$$\chi^\sigma_{00} = \frac{1}{\sqrt{2}}(\alpha\beta - \beta\alpha),$$

Preprints (www.preprints.org) | NOT PEER-REVIEWED | Posted: 19 October 2023 doi:10.20944/preprints202310.1221.v1

Coupling the spin wave functions of two sub-clusters by Clebsch-Gordan coefficients, total spin wave function can be written below,

$$
\begin{aligned}
|S_1\rangle &= \chi_0^{\sigma 1} = \chi_{00}^{\sigma}\chi_{00}^{\sigma}, \\
|S_2\rangle &= \chi_0^{\sigma 2} = \sqrt{\frac{1}{3}}(\chi_{11}^{\sigma}\chi_{1-1}^{\sigma} - \chi_{10}^{\sigma}\chi_{10}^{\sigma} + \chi_{1-1}^{\sigma}\chi_{11}^{\sigma}), \\
|S_3\rangle &= \chi_1^{\sigma 1} = \chi_{00}^{\sigma}\chi_{11}^{\sigma}, \\
|S_4\rangle &= \chi_1^{\sigma 2} = \chi_{11}^{\sigma}\chi_{00}^{\sigma}, \\
|S_5\rangle &= \chi_1^{\sigma 3} = \frac{1}{\sqrt{2}}(\chi_{11}^{\sigma}\chi_{10}^{\sigma} - \chi_{10}^{\sigma}\chi_{11}^{\sigma}), \\
|S_6\rangle &= \chi_2^{\sigma 1} = \chi_{11}^{\sigma}\chi_{11}^{\sigma}.
\end{aligned}
$$

The total spin wave function is denoted by $\chi_S^{\sigma i}$, i is the index of the functions, the S is the total spin of the system.

2.2.3. flavor wave function

We have two flavor wave functions of the system,

$$
\begin{aligned}
|F_1\rangle &= (s\bar{s})(s\bar{s}), \\
|F_2\rangle &= (ss)(\bar{s}\bar{s}).
\end{aligned}
$$

$|F_1\rangle$ is for meson-meson structure, and $|F_2\rangle$ is for diquark-antidiquark structure.

2.2.4. color wave function

The colorless tetraquark system has four color wave functions, two for meson-meson structure, $1 \otimes 1$ (C_1), $8 \otimes 8$ (C_2), and two for diquark-antidiquark structure, $\bar{3} \otimes 3$ (C_3) and $6 \otimes \bar{6}$ (C_4).

$$
\begin{aligned}
|C_1\rangle &= \sqrt{\frac{1}{9}}(\bar{r}r\bar{r}r + \bar{r}r\bar{g}g + \bar{r}r\bar{b}b + \bar{g}g\bar{r}r + \bar{g}g\bar{g}g \\
&\quad + \bar{g}g\bar{b}b + \bar{b}b\bar{r}r + \bar{b}b\bar{g}g + \bar{b}b\bar{b}b), \\
|C_2\rangle &= \sqrt{\frac{1}{72}}(3\bar{b}r\bar{r}b + 3\bar{g}r\bar{r}g + 3\bar{b}g\bar{g}b + 3\bar{g}b\bar{b}g + 3\bar{r}g\bar{g}r \\
&\quad + 3\bar{r}b\bar{b}r + 2\bar{r}r\bar{r}r + 2\bar{g}g\bar{g}g + 2\bar{b}b\bar{b}b - \bar{r}r\bar{g}g \\
&\quad - \bar{g}g\bar{r}r - \bar{b}b\bar{g}g - \bar{b}b\bar{r}r - \bar{g}g\bar{b}b - \bar{r}r\bar{b}b), \\
|C_3\rangle &= \sqrt{\frac{1}{12}}(rg\bar{r}\bar{g} - rg\bar{g}\bar{r} + gr\bar{g}\bar{r} - gr\bar{r}\bar{g} + rb\bar{r}\bar{b} \\
&\quad - rb\bar{b}\bar{r} + br\bar{b}\bar{r} - br\bar{r}\bar{b} + gb\bar{g}\bar{b} - gb\bar{b}\bar{g} \\
&\quad + bg\bar{b}\bar{g} - bg\bar{g}\bar{b}), \\
|C_4\rangle &= \sqrt{\frac{1}{24}}(2rr\bar{r}\bar{r} + 2gg\bar{g}\bar{g} + 2bb\bar{b}\bar{b} + rg\bar{r}\bar{g} + rg\bar{g}\bar{r} \\
&\quad + gr\bar{g}\bar{r} + gr\bar{r}\bar{g} + rb\bar{r}\bar{b} + rb\bar{b}\bar{r} + br\bar{b}\bar{r} \\
&\quad + br\bar{r}\bar{b} + gb\bar{g}\bar{b} + gb\bar{b}\bar{g} + bg\bar{b}\bar{g} + bg\bar{g}\bar{b}).
\end{aligned} \tag{12}
$$

Preprints (www.preprints.org) | NOT PEER-REVIEWED | Posted: 19 October 2023 doi:10.20944/preprints202310.1221.v1

2.2.5. total wave function

The total wave functions are obtained by the direct product of wave functions of orbital, spin, color and flavor wave functions. Because we are interested in the states with positive parity, there are three quantum number: 0^+, 1^+, and 2^+. Finally, the total wave function of the system is written as:

$$\Psi^{i,j,k}_{JM_J} = \mathcal{A}\left[\left[\psi_L \chi^{\sigma_i}_S\right]_{JM_J} \chi^{fi}_j \chi^{ci}_k\right]. \tag{13}$$

At last, we solve the following Schrödinger equation to obtain eigen-energies of the system, with the help of the Rayleigh-Ritz variational principle.

$$H\Psi^{i,j,k}_{JM_J} = E\Psi^{i,j,k}_{JM_J}, \tag{14}$$

where $\Psi^{i,j,k}_{JM_J}$ is the wave function of the four-quark states, which is the linear combinations of the above channel wave functions.

3. Real-scaling method

The real-scaling method, originally introduced by Taylor [27] to estimate the energies of long-lived metastable states of electron-atom, electron-molecule, and atom-diatom complexes, has since found applications in resonance state studies. Jack Simons [28] extended this method to investigate resonance states. Emiko Hiyama *et al.* [29] were among the first to apply the real-scaling method within a quark model context to search for P_c states in the $qqqc\bar{c}$ system.

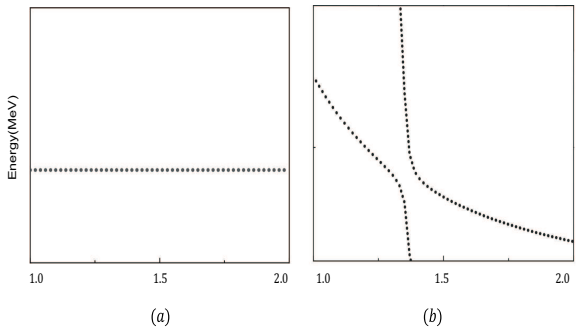

Figure 1. Two forms of resonant states (a) the resonance has weak coupling (or no coupling) with the scattering states; (b) the resonances has strong coupling with the scattering states;

Distinguished from other resonance computation methods based on stabilized eigenvectors, the real-scaling method allows for the direct estimation of decay widths from the stabilization graph. In this approach, a scaling factor α is employed to adjust the finite volume. False resonant states, reproduced by superabundant colorful subclusters (molecular hidden-color state or diquark structure), fall down to the corresponding threshold. Genuine resonances, on the other hand, persist after coupling to the scattering states and remain stable as α increases. Genuine resonances manifest in two distinct forms:

(1)Weak Coupling: If the energy of a scattering state significantly differs from that of the resonance, indicating weak or no coupling between the resonances and scattering states, the resonance appears as a stable straight line.

(2)Strong Coupling: When the energy of a scattering state approaches that of the resonance, indicating strong coupling, an avoid crossing structure manifests between two declining lines.

The decay width can be estimated from the slopes of the resonance and scattering states using Eq. (15), where S_r denotes the slope of the resonance, S_s denotes the slope of the scattering state, and

Preprints (www.preprints.org) | NOT PEER-REVIEWED | Posted: 19 October 2023 doi:10.20944/preprints202310.1221.v1

α_c represents the energy level difference between the resonance and the scattering state. Furthermore, as α increases continually, the avoid crossing structure repeats, providing valuable insights into the resonance behavior.

$$\Gamma = 4|V(\alpha_c)|\frac{\sqrt{|S_r||S_s|}}{|S_r - S_s|} \tag{15}$$

4. Results and discussions

In this section, we present the numerical results obtained from our calculations, with a primary focus on the quest for potential resonance states within the $s\bar{s}s\bar{s}$ system possessing positive parity. As an initial step in our investigation, we conduct a dynamic calculation utilizing the Gaussian Expansion Method (GEM) to ascertain the presence of any bound states. By analyzing the energy levels of the diquark and color-octet structure, we aim to determine the potential for resonance states within the system. Subsequently, after extracting the energies through the generalized eigen-equation, we apply the real-scaling method to verify the stability of the computed energy levels. This methodology enables us to confirm whether the obtained energy levels indeed correspond to stable states.

4.1. Tetraquark States Analysis and Resonance Identification

In this subsection, we present a comprehensive analysis of all conceivable $s\bar{s}s\bar{s}$ tetraquark states with positive parity. The details of these states are summarized in Table 2, which includes the indices of orbit, flavor, spin, and color wave functions for each channel. Additionally, the Table provides information on the energy, threshold, and binding energy for each physical channel. Our analysis focuses on rigorously assessing the binding energy (E_B) of each color-singlet state by comparing its theoretical calculated value with its corresponding threshold value ($E_B = E_{th} - E$). If E_B is less than 0, we will manually set it to 0. It is noteworthy that color-excited states (color-octet and diquark structure) inherently possess internal attraction due to color interactions, so we omit the E_B values for the color-excited structures. Subsequently, we employ the real-scaling method to investigate whether states displaying attractive interactions, encompassing both color-excited and color-singlet states with E_B values less than zero, can indeed form resonance states. Since we are only interested in the resonant states below 3 GeV, resonance states with energies higher than 3 GeV are not considered.

Preprints (www.preprints.org) | NOT PEER-REVIEWED | Posted: 19 October 2023 doi:10.20944/preprints202310.1221.v1

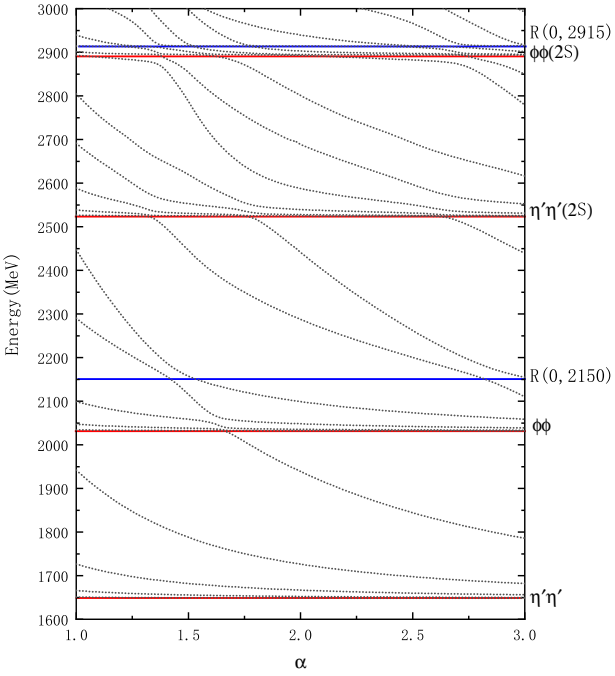

Figure 2. Energy spectrum of $J^P = 0^+$ states. The blue line depicts the resonant state, while the red line represents the physical threshold.

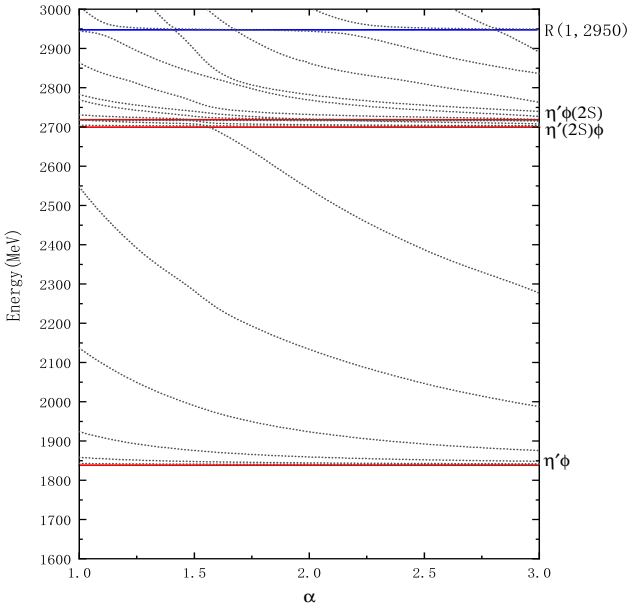

Figure 3. Energy spectrum of $J^P = 1^+$ states. The blue line depicts the resonant state, while the red line represents the physical threshold.

.

Preprints (www.preprints.org) | NOT PEER-REVIEWED | Posted: 19 October 2023 doi:10.20944/preprints202310.1221.v1

Table 2. The results for system with positive charity. The "$[meson]_8$" donates molecular color-octet state. "$[sub\text{-}diquark]^{spin}_{color}$" denotes diquark state, and "$[sub\text{-}antidiquark]^{spin}_{anti-color}$" denotes antidiquark state. The abbreviation "c.c.s.c" stands for "coupled-color-singlet-channels", "c.c.e.c" stands for "coupled-color-excited-channels", and "c.c.a.c" stands for "Complete coupled-all-channels". (unit: MeV)

$\|R_iF_jS_kC_n\rangle$	Channel	E	E^{Theo}_{th}	E_B	E^{Exp}_{th}
		$J^P = 0^+$			
$\|R_1F_1S_1C_1\rangle$	$\eta'\eta'$	1650	1648	0	1916
$\|R_1F_1S_2C_1\rangle$	$\phi\phi$	2032	2031	0	2040
c.c.s.c		1648			
$\|R_1F_1S_1C_2\rangle$	$[\eta']_8[\eta']_8$	2324			
$\|R_1F_1S_2C_2\rangle$	$[\phi]_8[\phi]_8$	2255			
$\|R_2F_2S_1C_4\rangle$	$[ss]^0_6[\bar{s}\bar{s}]^0_{\bar{6}}$	2298			
$\|R_2F_2S_2C_3\rangle$	$[ss]^1_3[\bar{s}\bar{s}]^1_{\bar{3}}$	2315			
c.c.e.c		2072			
c.c.a.c		1648			
		$J^P = 1^+$			
$\|R_1F_1S_3C_1\rangle$	$\eta'\phi$	1841	1840	0	1978
$\|R_1F_1S_4C_1\rangle$	$\phi\eta'$	1841	1840	0	1978
c.c.s.c		1841			
$\|R_1F_1S_3C_2\rangle$	$[\eta']_8[\phi]_8$	2247			
$\|R_1F_1S_4C_2\rangle$	$[\phi]_8[\eta']_8$	2247			
$\|R_2F_2S_5C_3\rangle$	$[ss]^1_3[\bar{s}\bar{s}]^1_{\bar{3}}$	2315			
c.c.e.c		2199			
c.c.a.c		1840			
		$J^P = 2^+$			
$\|R_1F_1S_6C_1\rangle$	$\phi\phi$	2032	2031	0	2040
c.c.s.c		2032			
$\|R_1F_1S_6C_2\rangle$	$[\phi]_8[\phi]_8$	2272			
$\|R_2F_2S_6C_3\rangle$	$[ss]^1_3[\bar{s}\bar{s}]^1_{\bar{3}}$	2315			
c.c.e.c		2242			
c.c.a.c		2031			

The $J^P = 0^+$ sector: Upon detailed analysis presented in Table 2, we observe a total of two color-singlet states, $\eta'\eta'$ and $\phi\phi$, existing in the 0^+ system. Additionally, their corresponding color-octet states and two diquark states are identified within an energy range of approximately 2.25-2.32 GeV. Remarkably, the result reveals that the color-singlet states ($\eta'\eta'$ and $\phi\phi$) do not form bound states, even if the channel coupling effect is taken into consideration. To further investigate and identify resonant states, we perform structure-coupling calculations, coupling the color excitation structure with the color-singlet structure using the real-scaling method. The results demonstrate a continuous decrease in energy as the factor α increases from its initial value of 1. At approximately $\alpha = 1.4$, a distinct avoid-crossing structure emerges, repeating at $\alpha = 2.7$, which represents the resonant state in our study. We denote it as $R(0, 2150)$ (we label the resulting resonant state with $R(J, energy)$). Analogously, we identify another resonance state, $R(0, 2915)$, positioned above the $\phi\phi(2S)$ energy level.

Preprints (www.preprints.org) | NOT PEER-REVIEWED | Posted: 19 October 2023 doi:10.20944/preprints202310.1221.v1

The $J^P = 1^+$ sector:In principle, a tetraquark system with a total spin of 1 should exhibit three possible combinations: 0×1, 1×0, and 1×1. These combinations, when combined with two types of spatial wave functions ($|R_1\rangle$, $|R_2\rangle$) and four types of color wave functions ($|C_1\rangle$, $|C_2\rangle$, $|C_3\rangle$, $|C_4\rangle$), result in a total of 12 channels for the wave function. However, due to symmetry constraints, the $s\bar{s}s\bar{s}$ tetraquark system with 1^+ spin is limited to only five channels: two color-singlet states ($\eta'\phi$, $\phi\eta'$), two corresponding color-octet states, and one diquark state. Our calculation results indicate that the $s\bar{s}s\bar{s}$ tetraquark system with 1^+ does not have any bound states. The energies of the color-excited structure are predominantly centered around 2.25 GeV. The evident coupling effect among these states is noteworthy, leading to a notable reduction in the minimum energy from 2.25 GeV to 2.20 GeV due to the influence of coupling channels. This state may be a potential candidate for $X(2100)$ in experimental observations. However, within the real-scaling framework, this state undergoes decay to the corresponding threshold, implying its non-existence in our study. Intriguingly, we have identified a stable structure at approximately 2.95 GeV, denoted as $R(1, 2950)$.

The $J^P = 2^+$ sector:For a tetraquark system with a total spin of 2, the available states are considerably reduced. In this scenario, there exists only one color-singlet state, $\phi\phi$. Additionally, a color-octet molecular state $[\phi]_8[\phi]_8$ and a diquark state $[ss]_3^1[\bar{s}\bar{s}]_{\bar{3}}^1$ are present, yielding a total of three wave functions. The energies of these states are primarily concentrated in the range of 2 GeV to 2.3 GeV. Intriguingly, resonance state calculations reveal a prominent resonance state, $R(2, 2850)$, as depicted in Figure 4.

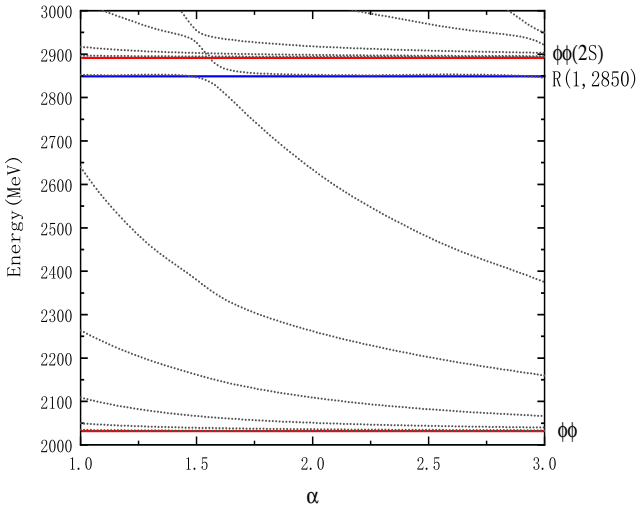

Figure 4. Energy spectrum of $J^P = 2^+$ states. The blue line depicts the resonant state, while the red line represents the physical threshold.

Table 3. The main component, width, and root-mean-square distances of resonances in $s\bar{s}s\bar{s}$ systems.

State	Main component	Width (MeV)	$r_{s\bar{s}}(fm)$	$r_{ss}(fm)$	$r_{\bar{s}\bar{s}}(fm)$
	$J^P = 0^+$				
$R(0, 2150)$	diquark structure(48%)+color-octet(50%)+the others.	65	0.87	0.94	0.94
$R(0, 2915)$	diquark structure(45%)+color-octet(51%)+the others.	45	0.98	1.11	1.26
	$J^P = 1^+$				
$R(1, 2950)$	diquark structure(41%)+color-octet(52%)+the others.	85	1.06	0.96	0.96
	$J^P = 2^+$				
$R(2, 2850)$	diquark structure(51%)+color-octet(48%)+the others.	90	1.01	0.77	0.77

Preprints (www.preprints.org) | NOT PEER-REVIEWED | Posted: 19 October 2023 doi:10.20944/preprints202310.1221.v1

From the comprehensive analysis discussed above, a total of four resonance states are identified: $R(0,2150)$, $R(0,2915)$, $R(1,2950)$, and $R(2,2850)$. These resonance states exhibit a root-mean-square distance concentrated around 1 fm and widths in the range of 40-90 MeV. This can be attributed to their predominant composition of diquark and color-octet states. Of particular interest is that $R(0,2915)$ and $R(1,2950)$ have energies slightly above the $\phi\phi(2S)$ threshold, resembling the characteristics of $X(6900)$, which resides just above the $J/\psi J/\psi(2S)$ threshold. This similarity suggests a possible kinship, positioning $R(0,2915)$ and $R(1,2950)$ as potential counterparts to $X(6900)$. Similarly, the energy of $R(0,2150)$ falls above $\phi\phi$ and below $\eta'\eta'(2S)$, resembling the energy characteristics of $X(6600)$. This observation leads to the hypothesis that $R(0,2150)$ could be a kin to $X(6600)$. On the other hand, $R(0,2150)$ also can be the candidate of $f_0(2100)$.

4.2. Compared With The Other Work

Table 4. The comparison of the energies of resonances in $s\bar{s}s\bar{s}$ systems with positive parity in different calculations (unit: MeV)

state	Ref.[19]	Ref.[21]	Ref.[[20]]	Ref.[23]	Ref.[22]
		$J^P = 0^+$			
$R(0,2150)$	1925	2110^{+19}_{-21}	2450^{+20}_{-24}	2218	-
$R(0,2915)$				2440	
				2781	
				2876	
				2948	
				3232	
		$J^P = 1^+$			
$R(1,2950)$	-	2060^{+18}_{-20}	-	2323	2080 ± 12
				2867	
				2954	
		$J^P = 2^+$			
$R(2,2850)$	-	2090^{+19}_{-22}	3070^{+25}_{-33}	2378	-
				2878	
				2963	
				2977	

As highlighted in our introduction, there has been some prior research on the $s\bar{s}s\bar{s}$ tetraquark system. This diverse body of work, encompassing various models and methods, not only check the model dependence of results but also contributes to a more profound comprehension of the $s\bar{s}s\bar{s}$ tetraquark system's nature. These research endeavors broadly fall into two categories: QCD sum rule and quark potential energy models. Our findings, as presented in Table 4, demonstrate qualitative consistency with previous calculations. For a quantum number of 0^+, our calculations yield two resonant states, namely $R(0,2150)$ and $R(0,2915)$. Remarkably, the energy of $R(2150)$ closely resembles the energy values reported in other studies. In Ref. [23], up to six energy levels are presented, one of which closely matches our $R(2915)$ energy value. Notably, the remaining potential energy levels between $R(2150)$ and $R(2915)$ in our calculations are found to decay into their corresponding threshold states, resulting in the identification of two resonance states. At a quantum number of 1^+, both QCD sum rule methods yield energies approximately around 2060 MeV [21,22], which is notably lower than the energy associated with $R(1,2950)$ in our findings. In fact, in our model's calculations,

 doi:10.20944/preprints202310.1221.v1

the energies of diquark structure also falls in the vicinity of 2200 MeV. However, it's important to note that strong channel coupling effects in our calculations lead to the decay of some energy levels into their respective threshold channels. On the other hand, the energy level of 2954 MeV in Ref.[23] closely corresponds to our result, $R(1,2950)$. In the case of a quantum number of 2^+, our energy level calculations exhibit significant similarities to the 1^+ quantum number scenario. The energy value associated with $R(2,2850)$ is in strong agreement with results reported in Refs.[20,23].

5. Summary

Within the framework of the quark model, we conducted a comprehensive study on the $s\bar{s}s\bar{s}$ system, exploring three different quantum number combinations, namely, $J^P = 0^+$, 1^+, and 2^+. Our investigations include not only the diquark structure but also molecular structures while accounting for all permissible color, flavor, and spin configurations.

The dynamic calculations yielded no bound states under any of the three quantum numbers. Nevertheless, the presence of color attraction mechanisms within the color-excited structures, encompassing both color-octet structures and diquark structures, introduced the possibility of several potential resonances. To ascertain the stability of these potential resonant states, we employed the real-scaling method. The results reveal that the majority of false resonances decayed into their corresponding threshold channels, leaving behind only four confirmed resonance states: two $J^P = 0^+$ resonances $R(0,2150)$, $R(0,2915)$, one $J^P = 1^+$ resonances $R(1,2950)$, and one $J^P = 2^+$ resonances $R(2,2850)$. These four resonant states share similar compositions, primarily dominated by diquark structures and color-octet structures. Consequently, they exhibit root-mean-square distances of around 1 fm and widths within the range of 40-90 MeV.

In conjunction with experimental insights from $c\bar{c}c\bar{c}$ systems, we draw parallels between our findings and the observed $X(6900)$, which has an energy slightly above that of $J/\psi J/\psi(2S)$ and a width several tens of MeV larger. Similarly, the energies of $R(0,2915)$ and $R(1,2950)$ in our results are slightly higher than that of $\phi\phi(2S)$ and possess widths exceeding 45 MeV, suggesting their potential kinship to $X(6900)$. Additionally, we propose that the $R(0,2150)$ which is the candidate of $f_0(2100)$ could be a cousin of $X(6600)$. Given the consistency between our calculations and the work of others, we recommend that experimental efforts explore the existence of these resonant states in the future.

Acknowledgments: This work is supported partly by the National Natural Science Foundation of China under Grant Nos. 12205249, 11675080, 11775118 and 11535005, and the Funding for School-Level Research Projects of Yancheng Institute of Technology (No. xjr2022039).

1. S. K. Choi *et al.* [Belle Collaboration], Phys. Rev. Lett. **91**, 262001 (2003).
2. B. Aubert *et al.* [BaBar], Phys. Rev. Lett. **95**, 142001 (2005) doi:10.1103/PhysRevLett.95.142001 [arXiv:hep-ex/0506081 [hep-ex]].
3. M. Ablikim *et al.* [BESIII], Phys. Rev. Lett. **110**, 252001 (2013) doi:10.1103/PhysRevLett.110.252001 [arXiv:1303.5949 [hep-ex]].
4. X. L. Wang *et al.* [Belle], Phys. Rev. Lett. **99**, 142002 (2007) doi:10.1103/PhysRevLett.99.142002 [arXiv:0707.3699 [hep-ex]].
5. J. He and P. L. Lü, Nucl. Phys. A **919**, 1-14 (2013) doi:10.1016/j.nuclphysa.2013.10.001 [arXiv:1309.6718 [hep-ph]].
6. Y. Tan, X. Liu, X. Chen, H. Huang and J. Ping, Phys. Rev. D **108**, no.1, 014017 (2023) doi:10.1103/PhysRevD.108.014017 [arXiv:2210.16250 [hep-ph]].
7. H. Huang, C. Deng, X. Liu, Y. Tan and J. Ping, Symmetry **15**, no.7, 1298 (2023) doi:10.3390/sym15071298
8. R. Aaij *et al.* [LHCb], Sci. Bull. **65**, no.23, 1983-1993 (2020) doi:10.1016/j.scib.2020.08.032 [arXiv:2006.16957 [hep-ex]].
9. L. Lunerti [CMS], PoS **ICHEP2022**, 941 doi:10.22323/1.414.0941
10. G. Aad *et al.* [ATLAS], Phys. Rev. Lett. **131**, no.15, 151902 (2023) doi:10.1103/PhysRevLett.131.151902 [arXiv:2304.08962 [hep-ex]].

11. B. Aubert *et al.* [BaBar], Phys. Rev. D **74**, 091103 (2006) doi:10.1103/PhysRevD.74.091103 [arXiv:hep-ex/0610018 [hep-ex]].
12. M. Ablikim *et al.* [BESIII], Phys. Rev. D **99**, no.11, 112008 (2019) doi:10.1103/PhysRevD.99.112008 [arXiv:1901.00085 [hep-ex]].
13. M. Ablikim *et al.* [BESIII], Phys. Rev. D **93**, no.11, 112011 (2016) doi:10.1103/PhysRevD.93.112011 [arXiv:1602.01523 [hep-ex]].
14. M. Ablikim *et al.* [BESIII], Phys. Rev. D **99**, no.3, 032001 (2019) doi:10.1103/PhysRevD.99.032001 [arXiv:1811.08742 [hep-ex]].
15. Z. G. Wang, Nucl. Phys. A **791**, 106-116 (2007) doi:10.1016/j.nuclphysa.2007.04.012 [arXiv:hep-ph/0610171 [hep-ph]].
16. H. X. Chen, X. Liu, A. Hosaka and S. L. Zhu, Phys. Rev. D **78**, 034012 (2008) doi:10.1103/PhysRevD.78.034012 [arXiv:0801.4603 [hep-ph]].
17. H. X. Chen, C. P. Shen and S. L. Zhu, Phys. Rev. D **98**, no.1, 014011 (2018) doi:10.1103/PhysRevD.98.014011 [arXiv:1805.06100 [hep-ph]].
18. Q. F. Lü, K. L. Wang and Y. B. Dong, Chin. Phys. C **44**, no.2, 024101 (2020) doi:10.1088/1674-1137/44/2/024101 [arXiv:1903.05007 [hep-ph]].
19. C. Deng, J. Ping, F. Wang and T. Goldman, Phys. Rev. D **82**, 074001 (2010) doi:10.1103/PhysRevD.82.074001
20. E. L. Cui, H. M. Yang, H. X. Chen, W. Chen and C. P. Shen, Eur. Phys. J. C **79**, no.3, 232 (2019) doi:10.1140/epjc/s10052-019-6755-y [arXiv:1901.01724 [hep-ph]].
21. N. Su and H. X. Chen, Phys. Rev. D **106**, no.1, 014023 (2022) doi:10.1103/PhysRevD.106.014023 [arXiv:2204.13959 [hep-ph]].
22. Z. G. Wang, Adv. High Energy Phys. **2020**, 6438730 (2020) doi:10.1155/2020/6438730 [arXiv:1901.04815 [hep-ph]].
23. F. X. Liu, M. S. Liu, X. H. Zhong and Q. Zhao, Phys. Rev. D **103**, no.1, 016016 (2021) doi:10.1103/PhysRevD.103.016016 [arXiv:2008.01372 [hep-ph]].
24. J. Vijande, F. Fernandez and A. Valcarce, J. Phys. G **31**, 481 (2005) doi:10.1088/0954-3899/31/5/017 [arXiv:hep-ph/0411299 [hep-ph]].
25. Y. Yang, C. Deng, H. Huang and J. Ping, Mod. Phys. Lett. A **23**, 1819-1828 (2008) doi:10.1142/S0217732308027102
26. Y. Tan, W. Lu and J. Ping, Eur. Phys. J. Plus **135**, no.9, 716 (2020) doi:10.1140/epjp/s13360-020-00741-w [arXiv:2004.02106 [hep-ph]].
27. Howard S. Taylor, Advan. Chem. Phys. **18**, 91-147(1970). doi:10.1002/9780470143650.ch3
28. J. Simons, J. Chem. Phys. **75**, 2465 (1981). doi:10.1063/1.442271
29. E. Hiyama, A. Hosaka, M. Oka and J. M. Richard, Phys. Rev. C **98**, no.4, 045208 (2018) doi:10.1103/PhysRevC.98.045208 [arXiv:1803.11369 [nucl-th]].